Simulation of Partially Obscured Scenes Using the Radiosity Method

by

Christoph C. Borel and Siegfried A.W. Gerstl

Space Science & Technology, SST-8, MS D438
Los Alamos National Laboratory
Los Alamos, New Mexico 87545, USA

Abstract

In this paper, the extended radiosity method or zonal method is used to construct realistic synthetic images (in the visible and infrared (IR)) containing radiatively participating media such as smoke, fog and clouds. Computational methods are discussed as well as the rendering of various scenes using computer graphics methods. The extended radiosity equations and an efficient algorithm to compute the radiosties and radiances in a homogeneous participating medium over an inhomogeneous flat surface are presented.

1 Introduction

The performance of IR sensors can be degraded by the presence of a participating medium between the sensor and the target. The contrast ratio between surfaces of different brightnesses is reduced by attenuation and multiple scattering in a participating medium. It is possible to simulate the image degradation due to smoke, fog and clouds by using 3-D radiative transfer calculations [1]. To date, the most common methods to solve radiative transfer (RT) equations are the discrete-ordinates method (DOM) [2] and the Monte-Carlo method [3]. In this paper we introduce the extended radiosity method as a means to generate synthetic images of partially obscured scenes. A major advantage of the radiosity method over the two RT methods is that very complex scene geometries can be analyzed. The radiosity method was originally developed by thermal engineers to calculate the radiative heat exchange between surfaces and a participating medium, e.g. in a furnace [4]. More recently the radiosity method has been applied to compute light intensities in complex environments with diffuse illumination [5, 6]. The emphasis was mostly to compute the multiple scattering between Lambertian surfaces. Some efforts have been made to extend the computer graphics radiosity method to include non-Lambertian surfaces and a participating medium. The current state of the art radiosity codes are able to handle almost 10^5 surfaces and volume elements on mid-size to super-computers [5, 6].

2 Extended Radiosity Method

The extended radiosity method for illuminated surfaces A_i and volume elements V_k is based on the two following coupled linear systems of equations for monochromatic radiation [4, 7] :

$$B_i^s\ A_i\ =\ E_i^s\ A_i\ +\ \rho_i \left[\sum_{j=1}^{N_s}\ B_j^s\ \underline{S_j\ S_i}\ +\ \sum_{k=1}^{N_v}\ B_k^v\ \underline{V_k\ S_i} \right]\ ,\quad i\ =\ 1, \ldots, N_s, \tag{1}$$

$$4\ \kappa_{t,k}\ B_k^v\ V_k\ =\ 4\ \kappa_{a,k}\ E_k^v\ V_k\ +\ \alpha_k \left[\sum_{j=1}^{N_s}\ B_j^s\ \underline{S_j\ V_k}\ +\ \sum_{m=1}^{N_v}\ B_m^v\ \underline{V_m\ V_k} \right]\ ,\quad k\ =\ 1, \ldots, N_v, \tag{2}$$

where B_i^s is the surface radiosity in $[W\ m^{-2}]$, E_i^s is the emission and ρ_i is the reflectance of surface patch i with area A_i. The flux density leaving a volume element k is given by $4\ \kappa_{t,k}\ B_k^v\ V_k$ where $\kappa_{t,k}$ is the sum of the absorption coefficient $\kappa_{a,k}$ and the scattering coefficient $\kappa_{s,k}$, and B_k^v is the volume radiosity. The scattering albedo of the k-th volume element is $\alpha_k\ =\ \kappa_{s,k}/\kappa_{t,k}$. The volume and surface radiosities are given by the sums of its emission and the scattered and reflected radiosities from all other surfaces and volumes. The fraction of energy reaching a surface or volume from another surface or volume through an absorbing medium is given by view factors. The view factor from a surface k to surface j is $\underline{S_k\ S_j}$, the view factor from volume k to surface i is $\underline{V_k\ S_i}$, the view factor from surface j to volume k is $\underline{S_j\ V_k}$, the view factor from volume m to volume k is $\underline{V_m\ V_k}$. The view factors depend on the geometry and attenuation of fluxes between elements and are usually difficult to evaluate.

Eqs. (1) and (2) assume that the surfaces are Lambertian reflectors so that the light is scattered equally into all directions. Three dimensional structures like clouds, fog and smoke can be simulated, by assigning absorption and scattering characteristics independently for each volume element V_k.

The view factor from surface k to surface j is defined as [4, 7] :

$$\underline{S_k\ S_j}\ =\ \int_{A_k} \int_{A_j} \frac{dA_k\ \cos\theta_k\ dA_j\ \cos\theta_j\ \tau(r)}{\pi\ r^2}. \tag{3}$$

The view factor from volume k to surface i is defined as [4, 7]:

$$\underline{V_k\ S_i}\ =\ \int_{V_k} \int_{A_i} \frac{\kappa_{t,k}\ dV_k\ dA_i\ \cos\theta_i\ \tau(r)}{\pi\ r^2}. \tag{4}$$

The view factor between volume m and volume k is defined as [4, 7] :

$$\underline{V_m\ V_k}\ =\ \int_{V_k} \int_{V_m} \frac{\kappa_{t,m}\ dV_m \kappa_{t,k}\ dV_k\ \tau(r)}{\pi\ r^2}. \tag{5}$$

The transmittance τ is given by :

$$\tau(r)\ =\ \exp\left[-\int_0^r\ \kappa_t(\chi)\ d\chi \right] \tag{6}$$

for a medium with variable κ_t along the line-of-sight path of length r.

3 Solution of the Radiosity Equations

The solution of eqs. (1,2) using eqs. (3- 5) can be obtained using the Gauss-Seidel iteration scheme. The following two eqs. show the mechanism :

$$B_i^{s,l+1} = E_i^s + \frac{\rho_i}{A_i} \sum_{k=1}^{N_v} B_k^{v,n} \underline{V_k\ S_i} - \frac{\rho_i}{A_i} \left[\sum_{j=1}^{i-1} B_j^{s,l+1} \underline{S_j\ S_i} + \sum_{j=i+1}^{N_s} B_j^{s,l} \underline{S_j\ S_i} \right], \quad i = 1, \ldots, N_s \tag{7}$$

$$B_k^{v,n+1} = \frac{\kappa_{a,k}}{\kappa_{t,k}} E_k^v + \frac{\alpha_k}{4\ \kappa_{t,k}\ V_k} \sum_{j=1}^{N_s} B_j^{s,l+1} \underline{S_j\ V_k} - \frac{\alpha_k}{4\ \kappa_{t,k}\ V_k} \left[\sum_{j=1}^{k-1} B_j^{v,n+1} \underline{V_j\ V_k} + \sum_{j=k+1}^{N_v} B_j^{v,n} \underline{V_j\ V_k} \right], \quad k = 1, \ldots, N_v \tag{8}$$

The superscripts l and n denote the iteration. The iteration ends when the absolute errors for the surface and volume radiosities fulfill the following criteria :

$$\mid B_i^{s,l+1} - B_i^{s,l} \mid < \varepsilon \text{ for all } i = 1, \ldots, N_s \tag{9}$$

and

$$\mid B_k^{v,n+1} - B_k^{v,n} \mid < \varepsilon \text{ for all } k = 1, \ldots, N_v. \tag{10}$$

The number of required iterations varies between 10 and 30 for most cases with an error limit of $\varepsilon = 10^{-9}$.

4 Rendering of Radiosity Solutions

The computed radiosities using eqs. (7) and (8) must be processed further in order to produce an image of the scene. The quantity a sensor measures is the radiance I which has the units of Watts per area per unit solid angle (e.g. $W\ m^{-2}\ sr^{-1}$). One can show that for Lambertian surfaces, the radiance is equal to the radiosity divided by π (e.g. [6]). The radiance from a surface behind a participating medium is attenuated by the transmission τ. The participating medium contributes additional radiance into the line of sight, with closer volume elements contributing more than more distant volume elements. The intensity of the light reaching the observer from a certain direction or along a ray is given by [7]:

$$I(L) = \tau(L) \frac{B_i^s}{\pi} + \int_0^L \tau(l) \frac{B^v(l)}{\pi} \kappa_t(l)\ dl, \tag{11}$$

$I(L)$ is the intensity on the outside of the imaged parallelepiped, L is the distance between the entrance point of a ray to the exit point at the detector location. If the exit point lies on the surface, the attenuated radiosity B_i^s must be added to the integral. The volume radiosity $B^v(l)$ along a ray from 0 to L can be approximated by a tri-linear interpolation of the discrete volume radiosities.

5 Scene Simulation Using the Extended Radiosity Method

To illustrate the use of the radiosity method, we chose a simple case where a parallelepiped of a homogeneous participating medium is located above a flat Lambertian surface. The surface consists of $N_s = N_x \times N_y$ rectangular patches with varying reflectance. The parallelepiped is divided into $N_v = N_x \times N_y \times N_z$ volume elements. As an illumination source, we chose a point source at infinity with illuminating rays from the direction $(\theta_s,\ \phi_s)$. The observer is located at $(x_0,\ y_0,\ ,z_0)$.

The radiosity eqs. (1) and (2) can be written for this case as :

$$\begin{aligned} B^s_{i_x,i_y}\ \Delta x\ \Delta y &= E^s_{i_x,i_y}\ \Delta x\ \Delta y \\ &+ \rho_{i_x,i_y} \sum_{k_x=1}^{N_x}\sum_{k_y=1}^{N_y}\sum_{k_z=1}^{N_z} B^v_{k_x,k_y,k_z}\ \underline{V_{k_x,k_y,k_z}\ S_{i_x,i_y}}, \quad \begin{array}{l} i_x = 1,\ldots,N_x \\ i_y = 1,\ldots,N_y \end{array} \end{aligned} \tag{12}$$

and

$$\begin{aligned} 4\ \kappa_t\ B^v_{k_x,k_y,k_z}\ \Delta x\ \Delta y\ \Delta z &= 4\ \kappa_t\ E^v_{k_x,k_y,k_z}\ \Delta x\ \Delta y\ \Delta z \\ &+ \alpha \left[\sum_{j_x=1}^{N_x}\sum_{j_y=1}^{N_y} B^s_{j_x,j_y}\ \underline{S_{j_x,j_y}\ V_{k_x,k_y,k_z}} \right. \\ &\left. + \sum_{m_x=1}^{N_x}\sum_{m_y=1}^{N_y}\sum_{m_z=1}^{N_z} B^v_{m_x,m_y,m_z}\ \underline{V_{m_x,m_y,m_z}\ V_{k_x,k_y,k_z}} \right], \\ & k_x = 1,\ldots,N_x;\ k_y = 1,\ldots,N_y;\ k_z = 1,\ldots,N_z \end{aligned} \tag{13}$$

where the volume/surface and surface/volume view (cf. eq. (4) factors are given by :

$$\underline{V_{k_x,k_y,k_z}\ S_{i_x,i_y}} = \underline{S_{i_x,i_y}\ V_{k_x,k_y,k_z}} = \frac{\kappa_t\ (\Delta x\ \Delta y\ \Delta z)^2\ k_z^2\ \tau(k_x,k_y,k_z;i_x,i_y)}{\pi\ \{[(k_x-i_x)\Delta x]^2 + [(k_x-i_x)\Delta x]^2 + [k_z\ \Delta z]^2\}^{\frac{3}{2}}} \tag{14}$$

with transmittance :

$$\tau(k_x,k_y,k_z;i_x,i_y) = \exp[-\kappa_t \sqrt{[(k_x-i_x)\Delta x]^2 + [(k_x-i_x)\Delta x]^2 + [k_z\ \Delta z]^2}]. \tag{15}$$

The volume/volume view factors according to eq. (5) are :

$$\underline{V_{m_x,m_y,m_z}\ V_{k_x,k_y,k_z}} \;=\; \underline{V_{k_x,k_y,k_z}\ V_{m_x,m_y,m_z}} \;= \\ \frac{\kappa_t^2\ (\Delta x\ \Delta y\ \Delta z)^2\ \tau(m_x,m_y,m_z;k_x,k_y,k_z)}{\pi\ \{[(k_x-m_x)\Delta x]^2+[(k_x-m_x)\Delta x]^2+[(k_z-m_z)\Delta z]^2\}^{\frac{3}{2}}}, \tag{16}$$

with transmittance :

$$\tau(k_x,k_y,k_z;m_x,m_y,m_z) \;=\; \exp\left\{\kappa_t\ \sqrt{[(k_x-m_x)\Delta x]^2+[(k_x-m_x)\Delta x]^2+[(k_z-m_z)\ \Delta z]^2}\right\}. \tag{17}$$

Note that symmetry and reciprocity cause the view factors to depend only on relative offsets between the surfaces and volume elements, e.g.

$$\underline{V_{5,6,10}\ S_{1,1}} \;=\; \underline{V_{6,7,10}\ S_{2,2}} \;=\; \underline{V_{10,11,10}\ S_{6,6}} \;=\; \ldots \text{ etc}$$

and

$$\underline{V_{5,6,10}\ V_{1,1,1}} \;=\; \underline{V_{6,7,11}\ V_{2,2,2}} \;=\; \underline{V_{10,11,12}\ V_{6,6,3}} \;=\; \ldots \text{ etc .}$$

Therefore, it is only necessary to compute view factors from a corner surface ($S_{1,1}$) or corner volume ($V_{1,1,1}$) to all other volume elements ($k_x = 2,\ldots,N_x;\ k_y = 2,\ldots,N_y;\ k_z = 2,\ldots,N_z$). Thus only $N_x\ N_y\ N_z - 1$ surface to volume view factors need to be computed and stored and not $[N_x\ N_y]^2\ N_z - 1$ surface to volume view factors. Similarly only $N_x\ N_y\ N_z - 1$ volume to volume view factors need to be computed and stored and not $[N_x\ N_y\ N_z]^2 - 1$ volume to volume view factors. The number of necessary multiplications N_{mult} in one iteration step is of the order of :

$$N_{mult} \;=\; (N_x\ N_y\ N_z)^2 + 2\ N_x^2\ N_y^2\ N_z. \tag{18}$$

From eq. (18) one can see that the required CPU time increases with the 6-th power of N, where N stands for the number of volume elements along one direction, and is a measure of the spatial grid subdivision. On the computers we used for this calculation, a CPU hour was necessary to solve problems with 14 x 14 x 14 volume elements. For more practical problems (e.g. 100 x 100 x 10 volume elements) it is necessary to reduce the number of multiplications to reach a solution in reasonable time. For participating media with a large scattering coefficient and a small number of vertical cells where $\Delta x = \Delta y = \Delta z$, the view factors for distant surfaces and volumes become very small. The view factors are proportional to the square of the inverse distance and the transmission is a negative exponential of the distance. Therefore it is possible to approximate the multiple scattering by considering only scattered light from nearby volumes or surfaces. This can be done by collecting radiosities only from a small parallelepiped of dimensions $M_x\ \Delta x \times M_y\ \Delta y \times M_z\ \Delta z$ centered around the volume element or above a surface patch. The radiosity problem using this method requires M_{mult} multiplications :

$$M_{mult} \;=\; N_x\ N_y\ N_z\ M_x\ M_y\ M_z \;+\; 2\ N_x\ M_x\ N_y\ M_y\ N_z, \tag{19}$$

which is considerably less than in eq. (19). To illustrate the improvement let $N_x = 100$, $N_y = 100$, $N_z = 10$ and $M_x = 10$, $M_y = 10$, $M_z = 4$. We ran this problem on a Sun IPC SparcStation which is rated at 15.8 MIPS and 1.7 MFLOPS and it took 22 minutes and 45 seconds for one iteration. Had we run the full radiosity solution it would have taken 200 times longer or about 22 CPU-days (without taking possible increases due to more disk swapping into account) for just one iteration. The full solution might have taken over a year to converge.

In summary, since we assumed a homogeneous participating medium we had to compute only view factors from one volume element to all others and from one surface to all volume elements. The surface to surface view factors are all zero because of the flat surface assumption. The solutions were rendered using eq.(11) to produce synthetic images (see Fig. 1) as a sample case. The participating medium had an absorption coefficient of $\kappa_a = 0.3$ and a total scattering coefficient $\kappa_t = 0.8$. The dimensions of a volume element were $\Delta x = \Delta y = 0.1$ and $\Delta z = 0.05$ with $N_x = N_y = N_z = 10$. The surface had a reflectance of $\rho = 0.3$ with a higher reflectance of $\rho = 0.6$ in a square in the middle for $i_x = 4, 5, 6, 7$ and $i_y = 4, 5, 6, 7$. The Gauss-Seidel iteration converged after 13 iterations with 73 CPU seconds. The rendering of the 300 by 300 image using 10 interpolated radiosities along the line of sight took 73 seconds to compute.

6 Conclusions

The extended radiosity method is shown to be practicable and useful to generate realistic scenes taking into account multiple scattering between surfaces and a participating volumetric medium, such as smoke or another obscurant. The effects of such obscurants on surface images would otherwise be difficult or impossible to compute with either the standard radiosity methods or the 3-D radiative transfer methods required to treat such problems.

References

[1] A. Zardecki, S.A.W. Gerstl, W.G. Tam, and J.F. Embury. Image-quality degradation in a turbid medium under partially incoherent illumination. *J. Opt. Soc. Am.*, A3:393–400, 1986.

[2] R.B. Myneni, G. Assrar, and S.A.W. Gerstl. Radiative transfer in three dimensional leaf canopies. *Transport Theory and Statistical Physics*, 19(3-5):205–250, 1990.

[3] G.I. Marchuk et. al. *The Monte-Carlo Methods in Atmospheric Optics.* Springer Verlag, Heidelberg-New York, 1980.

[4] H.C. Hottel and A.F. Sarofim. *Radiative Transfer.* McGraw-Hill Book Company, New York, New York, 1967.

[5] D. Greenberg. Light reflection models for computer graphics. *Science*, 244:166–173, 1989.

[6] C.C. Borel, S.A.W. Gerstl, and B.J. Powers. The radiosity method in optical remote sensing of structured 3-d surfaces. *Rem. Sens. Environ.*, in print, 1991.

[7] H.E. Rushmeier and K.E. Torrance. The zonal method for calculating light intensities in the presence of a participating medium. *SIGGRAPH Proceedings*, 21(4):293, July 1987.

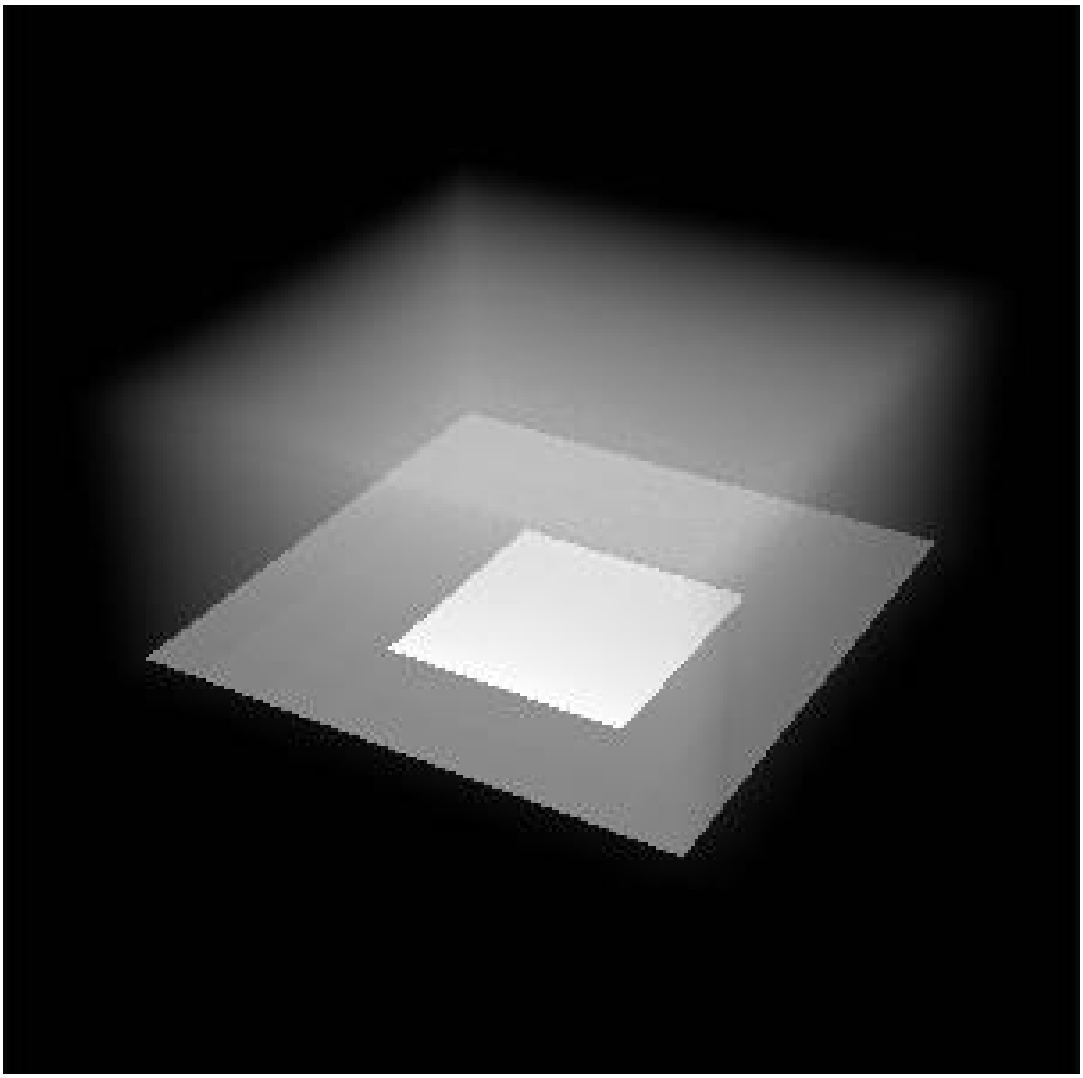

Figure 1. Synthetic image of a scene obscured by a participating medium.